Hindawi
Mathematical Problems in Engineering
Volume 2022, Article ID 5984177, 12 pages
https://doi.org/10.1155/2022/5984177

Research Article

Numerical Investigation on Shear Performance of Reinforced Concrete Beam by Using Ferrocement Composite

Edosa Megarsa[1] **and Goshu Kenea**[2]

[1]*Civil Engineering Department, College of Engineering and Technology, Ambo University, Ambo, Oromia, Ethiopia*
[2]*Civil Engineering Department, Jimma Institute of Technology, Jimma University, Jimma, Oromia, Ethiopia*

Correspondence should be addressed to Goshu Kenea; goshukeneatujuba@gmail.com

Received 18 February 2022; Revised 10 April 2022; Accepted 13 April 2022; Published 27 April 2022

Academic Editor: Piero Colajanni

This study presents an extensive analytical investigation of the shear performance of reinforced concrete beams by using ferrocement composite as transverse reinforcement. Nonlinear finite element simulation was conducted in Abaqus 6.14 software package. Fifteen beam models were selected under two-point loading. The main parameters considered includes the diameter, spacing, number of layers of wire mesh, and its combination with stirrups. The results testified that as the diameter and number of layers of wire mesh increased, the ultimate failure load, shear capacity, and stiffness of the model specimen also increased. However, as the number of layers becomes greater than three, no significant change happens in the shear performance of the beam. In another way, the failure load, shear capacity, and stiffness of the beam models are decreased, as the spacing between wire mesh is increased. Furthermore, the study confirmed that under the same weight criteria, the shear performance of RC beam specimens with wire mesh and its combination with stirrups as shear reinforcement is greater than specimens with stirrups only. Finally, the sensitivity analysis is conducted in MS excel to access the effect of each independent variable on the ultimate failure load of the RC beam.

1. Introduction

Structures made from concrete needed to be reinforced using different materials to improve their weak properties under tension force because concrete is good in compression but weak in tension. Now a days in the world, different technologies are being developed in the construction industry, and one of them is using simple and easily available materials to have a safe and economical building. Shear reinforcement needs more special attention than flexure failure because its failure does not show any warning. The replacement of stirrups by ferrocement (wire mesh) is mainly a reason for its high tensile and flexibility strength. Ferrocement is a closely spaced small diameter wire mesh, which needs a guiding principle in designing concrete structures as proposed in the ACI committee 549 [1].

A different investigation has been conducted both numerically and experimentally to access the effect of using ferrocement in different structures-like columns, column-beam joints, slabs, channels, and hollow beams to improve the shear performance under different types of loading [2–8]. In those studies, the ferrocement was used by replacing in place of transverse (stirrups) and longitudinal steel reinforcement. The investigation confirmed a significant increase in flexural and shear strength when the ferrocement was incorporated. This is caused due to high tensile strength, ductility, and flexibility as compared to normal steel reinforcement. On another hand, the performance of ferrocement in the composite beam was studied both experimentally and numerically under two-point loading [9]. The composite beam with ferrocement showed a good performance in terms of ultimate capacity, ductility, and cracking strength as compared to the control beam with normal reinforcement. A research study [10] was also conducted to strengthen and repair the reinforced concrete beam with ferrocement laminates. The study testified to a

significant improvement of flexural and shear strength when the beam is strengthened with wire mesh under cyclic loading. In addition, an experimental investigation was undertaken to evaluate the shear performance of concrete beams reinforced with steel fibers under monotonic and cyclic loading [11]. The study concluded that the beam with steel fibers showed ameliorated crack patterns, enhanced energy dissipation capacity, and high shear capacity.

In addition, the shear behavior of reinforced concrete box beams was studied using composite fabric as shear reinforcement [12]. This experimental investigation considered seven box beams under two-point loading. The beam with tensar wire mesh as transverse reinforcement exhibited an increase in ultimate failure load and shear capacity. In a similar way, the shear performance of RC box beams was studied with welded wire mesh and transverse reinforcement, both experimentally and analytically [13], which showed an improved shear performance compared to the control. Wire mesh has also wide applicability in different structural elements like RC column [14], rather than RC beam. In this study, expanded, welded, tensar, and fiberglass wire mesh were used as transverse reinforcement for the column test specimen. A column with wire mesh showed a good shear performance than the control beam with normal reinforcement.

Furthermore, a shear behavior of slender box beams was studied with ferrocement both experimentally and numerically in terms of cracking loading, ultimate loading, and deflection when subjected to loading [15]. In this study, mortar compressive strength and wire mesh were used as study parameters. Recently, an extensive experimental study was conducted to improve the shear performance of concrete beams with ferrocement composite [16]. In the study, a normal reinforced concrete beam was compared with beam ferrocement as shear reinforcement based on an equal weight ratio. Beam with ferrocement composite showed a good shear performance under two-point loading. However, further investigation is needed on the application of ferrocement composite in the concrete structural element because this material is a very cheap construction material in terms of cost and has good performance under the same condition as compared to steel reinforcement. In this study, the diameter, spacing, and the number of layers of wire mesh are considered as study parameters to access its effect on ultimate failure, shear capacity, and stiffness of reinforced concrete beam specimens. From the authors' knowledge, the diameter, spacing, and the number of layers of wire mesh were not considered as study parameters in accessing the shear performance of reinforced concrete beams yet. For this particular investigation, nonlinear finite element simulation was conducted in Abaqus 6.14, which has the capability of capturing both material and geometric nonlinearity.

2. FE Modeling

Nowadays, FE modeling is becoming the most impressive tool in studying structural behavior. It has the capability of capturing both material nonlinearity of concrete and steel and geometric nonlinearity under any type of loading (monotonic or cyclic loading). This particular study considered the Concrete Damaged Plasticity model [17] to investigate the shear performance of RC beam with ferrocement composite as shear reinforcement. The result obtained from FE simulation is mainly affected by the mathematical model employed to represent the stress-strain response of concrete for both tension and compression. The elastic properties of concrete cylindrical compressive strength of 25 MPa with 2,400 kg/m^3 unit weight, 0.2 Poisons ratio, and 31,476 MPa elastic modulus were used according to [18]. Not only the stress-strain response of the materials but also the type of interaction, boundary condition, meshing size, and type of loading have a significant effect on the FE simulation result.

2.1. Material Modeling

2.1.1. Uniaxial Concrete Compressive Modeling. The Concrete Damage Plasticity model needs a concrete uniaxial compressive stress-strain and compressive damage parameters as input to perform modeling in FE simulation. Different mathematical models are available and may be used to get the stress-strain response of concrete under uniaxial compression. This study employed the mathematical model proposed in Eurocode 2 [18] to obtain the concrete compressive stress-strain, as illustrated in Figure 1 and Equation (1) through (6). The concrete stress-strain response is assumed to be linear up to 40% of the ultimate compressive strength and nonlinear for the next segments of the curve.

$$\frac{\sigma_c}{f_{cm}} = \frac{k\eta - \eta^2}{1 + (k-2)\eta}, \tag{1}$$

$$f_{cm} = f_{ck} + 8\left(\frac{N}{mm^2}\right), \tag{2}$$

$$k = 1.05E_{cm}\left(\frac{\varepsilon_{c1}}{f_{cm}}\right), \tag{3}$$

$$\eta = \frac{\varepsilon_i}{\varepsilon_{c1}}, \tag{4}$$

$$\varepsilon_{c1} = 0.7f_{cm}^{0.32} < 2.8, \tag{5}$$

$$E_{cm} = 22\left[\frac{f_{cm}}{10}\right]^{0.3}, \tag{6}$$

2.1.2. Uniaxial Concrete Tensile Modeling. The tensile behavior of concrete was modeled in terms of stress versus cracking width or opening. The mathematical model proposed in [19] was employed as indicated in Figure 2 and Equation (7) through (10).where w is the cracking opening in mm; G_f is the fracture energy in N/mm^2; f_{ctm} is the

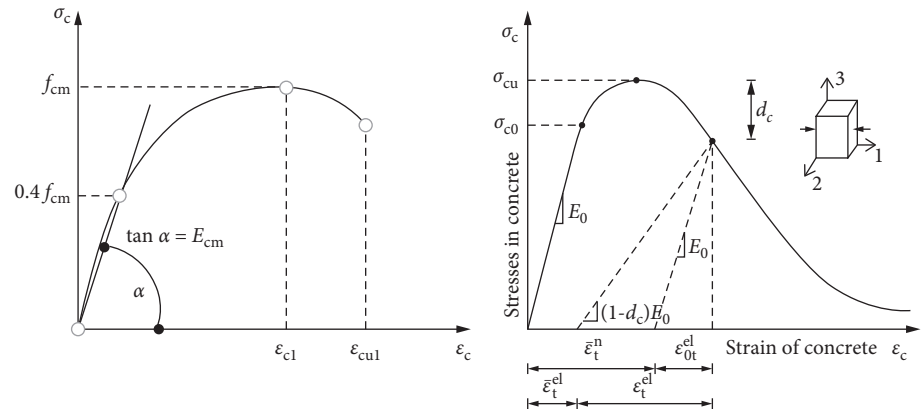

Figure 1: Concrete compressive stress-strain mathematical model.

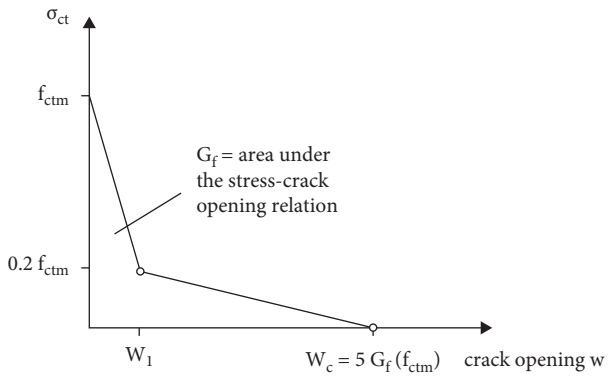

Figure 2: Tensile stress versus cracking width of concrete for the FE simulation.

ultimate tensile strength in N/mm^2; and f_{cm} is the concrete cylindrical compressive strength in N/mm^2.

$$\sigma_{ct} = f_{ctm}\left(1 - 0.8\frac{w}{w_1}\right) \text{for } w \le w_1, \tag{7}$$

$$\sigma_{ct} = f_{ctm}\left(0.25 - 0.05\frac{w}{w_1}\right) \text{for } w_1 < w \le w_c, \tag{8}$$

$$w_1 = \frac{G_f}{f_{ctm}}, \quad w_c = 5\frac{G_f}{f_{ctm}}, \ \&G_f = 73 f_{cm}^{0.18}, \tag{9}$$

$$f_{ctm} = \begin{cases} 0.3 * \left(f_{cm} - 8\right)^{2/3}, & \text{for } f_{cm} \le 58\dfrac{N}{mm^2}, \\ 2.12 * ln\left(1 + \left(\dfrac{f_{cm}}{10}\right)\right), & \text{for } f_{cm} > 58\dfrac{N}{mm^2}. \end{cases} \tag{10}$$

2.1.3. Concrete Damage Model. The concrete damage model includes cracking strain, crushing strain, tensile plastic strain, compressive plastic strain, tensile damage parameter (dt), and compressive damage parameter (dc), in which Equation (11) through (16) were used [17].

Table 1: Concrete damage parameters used for the model.

Eccentricity (γ)	Dilation angle (ψ)	K	σ_{bo}/σ_{co}	Viscosity parameter
0.1	36	0.667	1.16	0.0001

$$\sigma_c = (1 - d_c)E_{co}\left(\varepsilon_c - \varepsilon_c^{pl}\right), \tag{11}$$

$$\varepsilon_c^{ch} = \varepsilon_c - \varepsilon_{oc}^{el} = \varepsilon_c - \frac{\sigma_c}{E_{co}}, \tag{12}$$

$$\varepsilon_c^{pl} = \varepsilon_c^{ch} - \frac{d_c}{1 - d_c}\frac{\sigma_c}{E_{co}}, \tag{13}$$

$$\sigma_t = (1 - d_t)E_{co}\left(u_t - u_t^{pl}\right), \tag{14}$$

$$u_t^{ck} = u_t - u_{ot}^{el} = u_t - \frac{\sigma_t}{E_{co}}, \tag{15}$$

$$u_t^{pl} = u_t^{ck} - \frac{d_t}{1 - d_t}\frac{\sigma_t}{E_{co}}. \tag{16}$$

2.1.4. Concrete Damage Parameters. The damage parameters have been collected from the previously conducted research [20–22], which is validated against the experimental result. The magnitude of each parameter was presented in Table 1.

2.1.5. Steel Reinforcement and Wire Mesh. All longitudinal reinforcement, shear reinforcement, and wire mesh were modeled using the bilinear elastoplastic model as presented in [23–25]. The first linear line starts from zero and ends at the yield point, and the second linear line starts from the yield point and ends at the ultimate capacity. Unit weight of 7,850 kg/m^3 was used for both steel bar and wire mesh modeling. Table 2 illustrates the physical properties of wire mesh and steel bar material employed in the FE simulation.

Table 2: Steel reinforcement and wire mesh properties.

Steel diameter (mm)	Yield strength (MPa)	Poisons ratio	Ultimate strength(MPa)	Ultimate strain (%)	Elastic modulus (GPa)
Φ12	500	0.3	540	10	200
Φ8	500	0.3	540	10	200
Φ6	500	0.3	540	10	200
Φ_{mesh} 1.5, 2, 2.5	400	0.3	600	13	200

Table 3: Cross-section detail of different specimens based on parameters.

No	Beam name (Specimens)	Long-reinforcement		Stirrups (mm)	Wire mesh		Layer
		Tens-	Compr-		Diameter (mm)	Spacing (mm)	
1	CB0	2Φ12	2Φ8	Φ6 c/c 150	no	no	no
2	BΦ1S1L1	2Φ12	2Φ8	no	1.5	8 × 8	1
3	BΦ2S1L1	2Φ12	2Φ8	no	2	8 × 8	1
4	BΦ3S1L1	2Φ12	2Φ8	no	2.5	8 × 8	1
5	BΦ3S1L2	2Φ12	2Φ8	no	2.5	8 × 8	2
6	BΦ3S1L2	2Φ12	2Φ8	no	2.5	8 × 8	2
7	BΦ1S2L1	2Φ12	2Φ8	no	1.5	11 × 11	1
8	BΦ2S2L1	2Φ12	2Φ8	no	2	11 × 11	1
9	BΦ3S2L1	2Φ12	2Φ8	no	2.5	11 × 11	1
10	BΦ1S2L2	2Φ12	2Φ8	no	1.5	11 × 11	2
11	BΦ1S2L3	2Φ12	2Φ8	no	1.5	11 × 11	3
12	BΦ1S2L4	2Φ12	2Φ8	no	1.5	11 × 11	4
13	BΦ2S3L1	2Φ12	2Φ8	no	2	15 × 15	1
14	BΦ3S3L2	2Φ12	2Φ8	no	2.5	15 × 15	2
15	BΦ2S1L1-1	2Φ12	2Φ8	Φ6 c/c 360	2	8 × 8	1

2.2. Geometry and Samples. The study focused on diameter, spacing, and the layer of wire mesh as study variables to investigate the shear performance of RC beam under two-point loading. Table 3 shows the number of RC beam model specimens simulated in FE software, Abaqus 6.14. A total of 15 model specimens were considered to answer the objectives of the study. All the beam model specimens have a constant geometric dimension of 100 mm × 150 mm × 1200 mm, which represent the width, depth, and length of specimens, respectively.

A plain concrete beam with a rectangular section was modeled using the three-dimensional, deformable, and extrusion method as illustrated in Figure 3(a). Longitudinal bar, rectangular closed stirrup, and steel wire mesh were modeled using deformable and wire planar line as presented in Figures 3(b)–3(d), respectively.

2.3. Part Assembling. An assembly is a collection of positioned part instances. To form an assembly that acts as one-part, steel reinforcement (longitudinal and shear reinforcement) and wire mesh were embedded in a plain concrete beam using embedded constraint. In addition, rigid plates were used for support and load application using the node contact method. Figure 4 presents a model specimen in which different parts are assembled into a single unit to act together during loading.

2.4. Step Analysis. The static general loading was selected under step analysis. The static general method has the capability of capturing both material and geometrical nonlinearity effects of subsequent steps.

2.5. Loading and Boundary Condition. Boundary condition plays an important role in getting accurate results or output from finite element simulation. Increasing two equal concentrated loads were applied at a reference point on a rigid loading plate, which is allowed to translate along the vertical direction and restrained in other directions until the shear capacity of the beam (shear failure). Furthermore, using a rigid support plate and a reference point pin, support boundary conditions ($u1 = 0$, $u2 = 0$ & $u3 = 0$) were applied at the left support end and roller support boundary conditions ($u1 = 0$ & $u2 = 0$) were applied at the right support end. Figure 5 illustrates the loading and boundary conditions of the study specimen.

2.6. Mesh Size and Element Type. In the Abaqus element library, there are different types of elements, like hexahedron, shell, triangular prism, and others. The size of the mesh was determined or fixed after several iterations when the magnitude of output was not further changed. Table 4 shows the type of element and mesh size employed for each instance.

2.7. FE Validation. Previously published or conducted experimental research [26] has been used to validate the finite element simulation before modeling and analyzing the study specimens. The specimen used for FE validation was designated by B-2 and B-4 in the study, in which stirrups and wire mesh were used as shear reinforcement, respectively. The model specimen has a geometric dimension of 100 mm × 150 mm × 1200 mm, which represents the width,

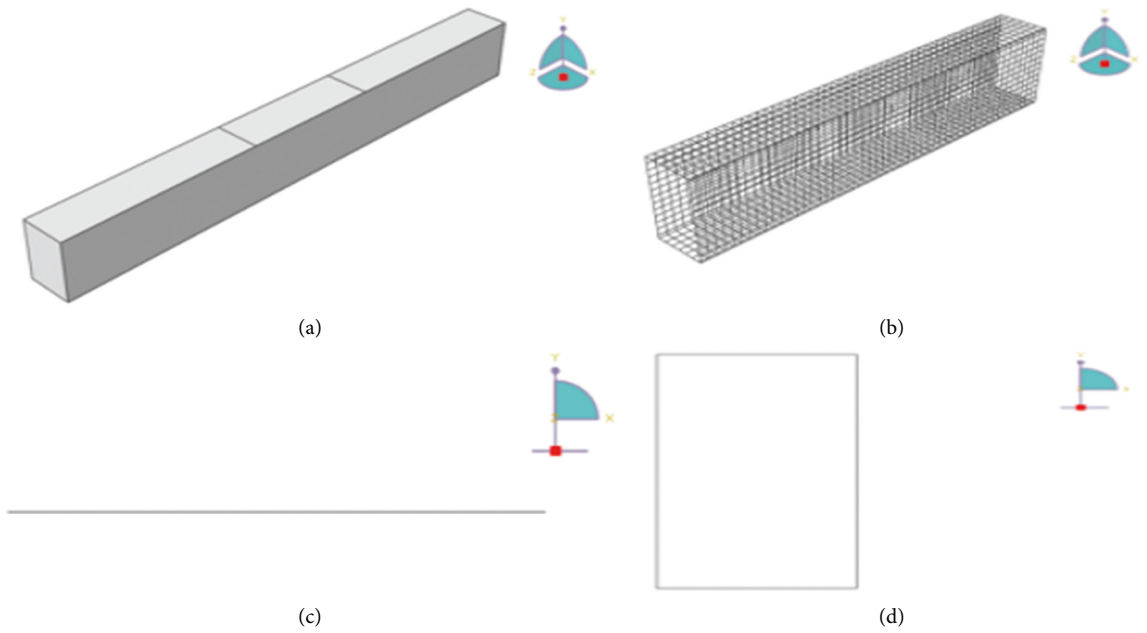

Figure 3: Geometric model for each parts (a) plain concrete beam; (b) wire mesh; (c) longitudinal bar; & (d) stirrup reinforcement).

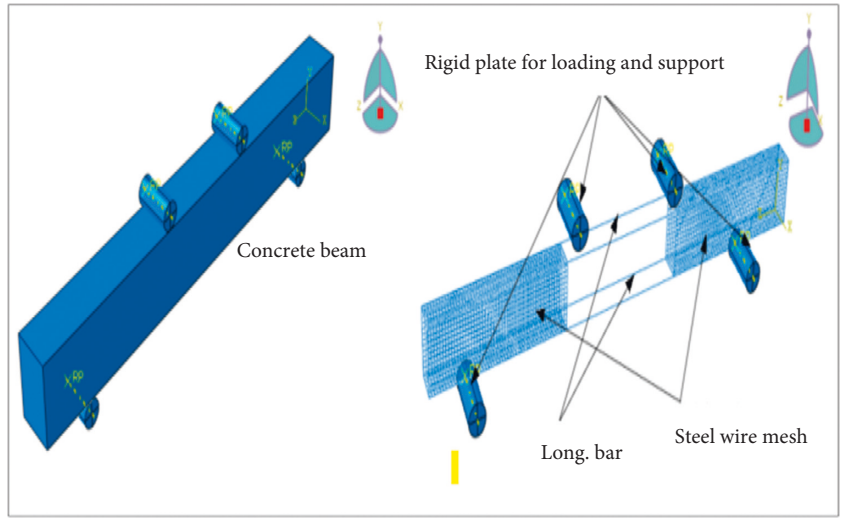

Figure 4: Assembling parts in FE simulation.

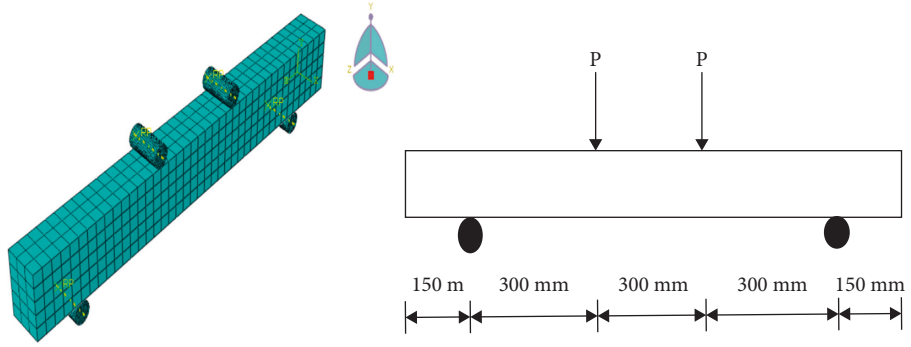

Figure 5: Boundary condition, loading, meshing, and length of beam.

Table 4: Mesh size and element type for each parts.

Parts	Concrete beam	Rigid plate	Wire mesh	Reinforcement bar
Mesh size (mm)	30	10	10	20
Element type	C3D8R	R3D4	T3D2	T3D2

Table 5: Comparison of experimental and FE result.

Category	Experimental results		Finite element results		Variation in percent	
Specimen	Failure load (kN)	Max. displacement (mm)	Failure load (kN)	Max. displacement (mm)	Failure load variation (%)	Displacement variation (%)
B-2	108.39	13.21	96.67	14.07	7.67	6.52
B-4	114.61	8.6	105.04	9.03	8.35	5

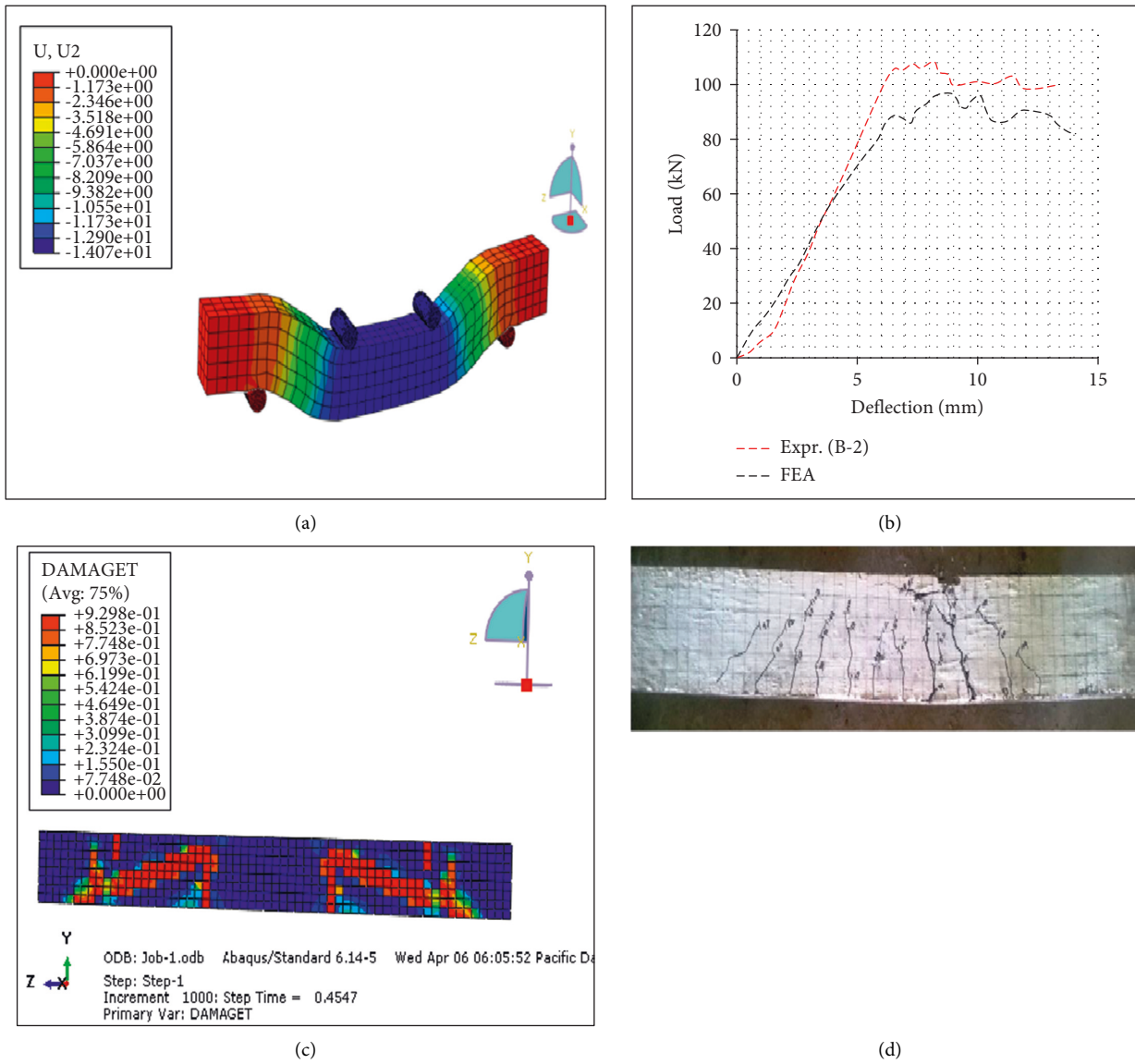

Figure 6: Comparison of experimental and FE result for B-2 with stirrups only (a) Deflection from FE analysis (b). Load vs. deflection response (c) Failure pattern from FE simulation (d) Failure pattern from experiment.

depth, and length of the beam, respectively. The beam was modeled in the FE software based on material properties, loading, and boundary condition conducted in the experimental test. The FE simulation result showed a good agreement with the experimental result. Table 5 presents the summary of finite element analysis and experimental results for both beam specimens with stirrups (B-2) and expanded wire mesh (B-4) as transverse reinforcement. In addition, Figures 6(a)–6(d) show the deflection from FE simulation, the comparison of load versus deflection between FE and experimental result, the failure pattern from FE simulation, and the failure pattern from the experimental test of B-2

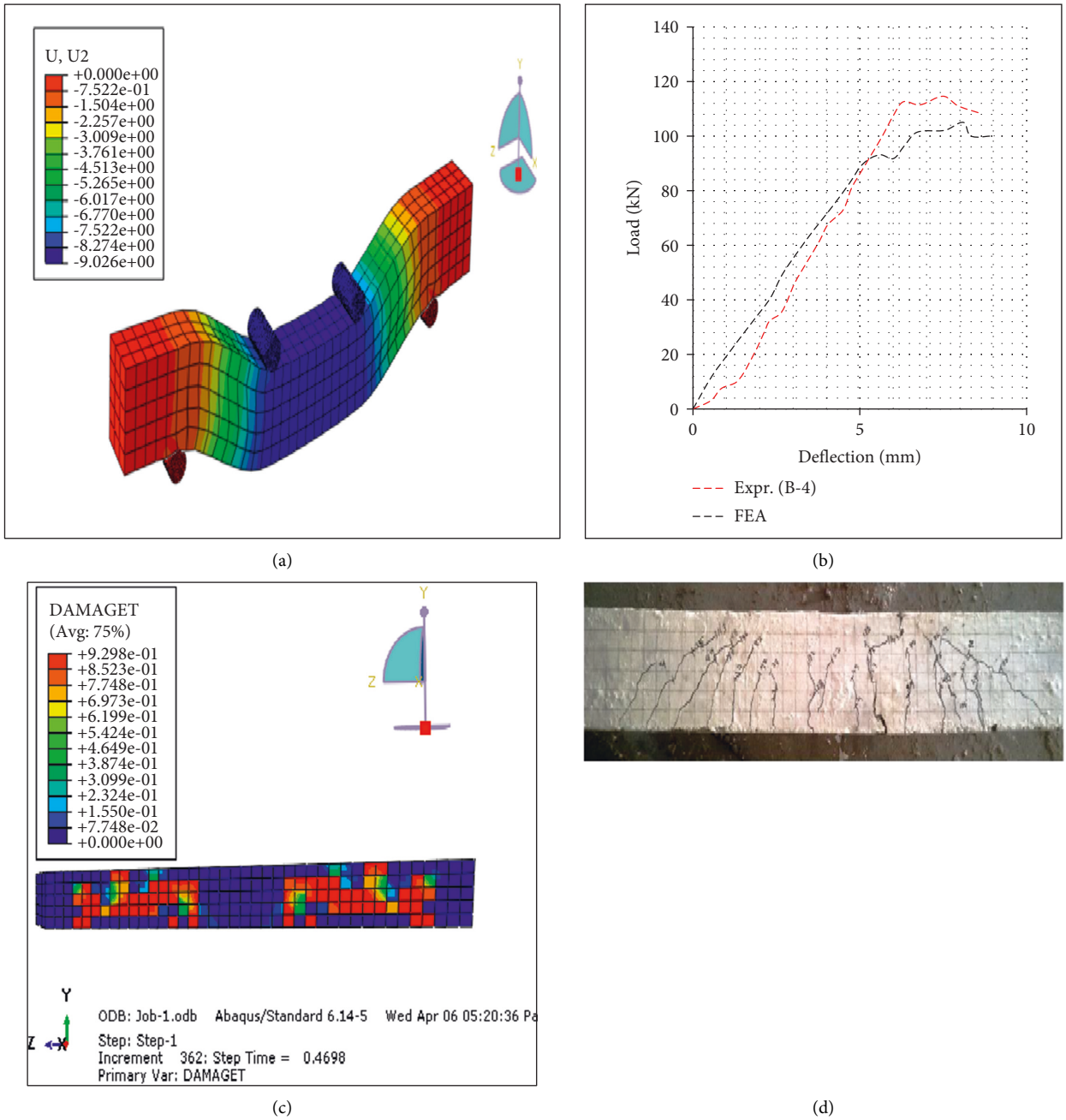

Figure 7: Comparison of experimental and FE result for B-4 with wire mesh only (a) Deflection from FE analysis (b). Load vs. deflection response (c) Failure pattern from FE simulation (d) Failure pattern from experiment.

model specimen, respectively, under increasing static loading. Furthermore, Figures 7(a)–7(d) show the deflection from FE simulation, the comparison of load versus deflection between FE and experimental result, the failure pattern from FE simulation, and the failure pattern from the experimental test of B-4 model specimen, respectively, under increasing static loading.

3. Result and Discussion

The finite element simulation result has been extracted based on the objective of the study. Figures 8(a)–8(d), illustrates a sample of FE results in terms of maximum shear stress, shear damage pattern, principal strain, and mid-deflection, respectively. The highlighted contour color was used to identify the most affected portion of model specimens under two-point loading.

3.1. Parametric Study

3.1.1. Effects of Diameter of Wire Mesh. In this study, the effect of changing the diameter of the wire mesh as a study parameter to investigate its influence on the failure load, shear stress, and stiffness of RC beam was detemined.

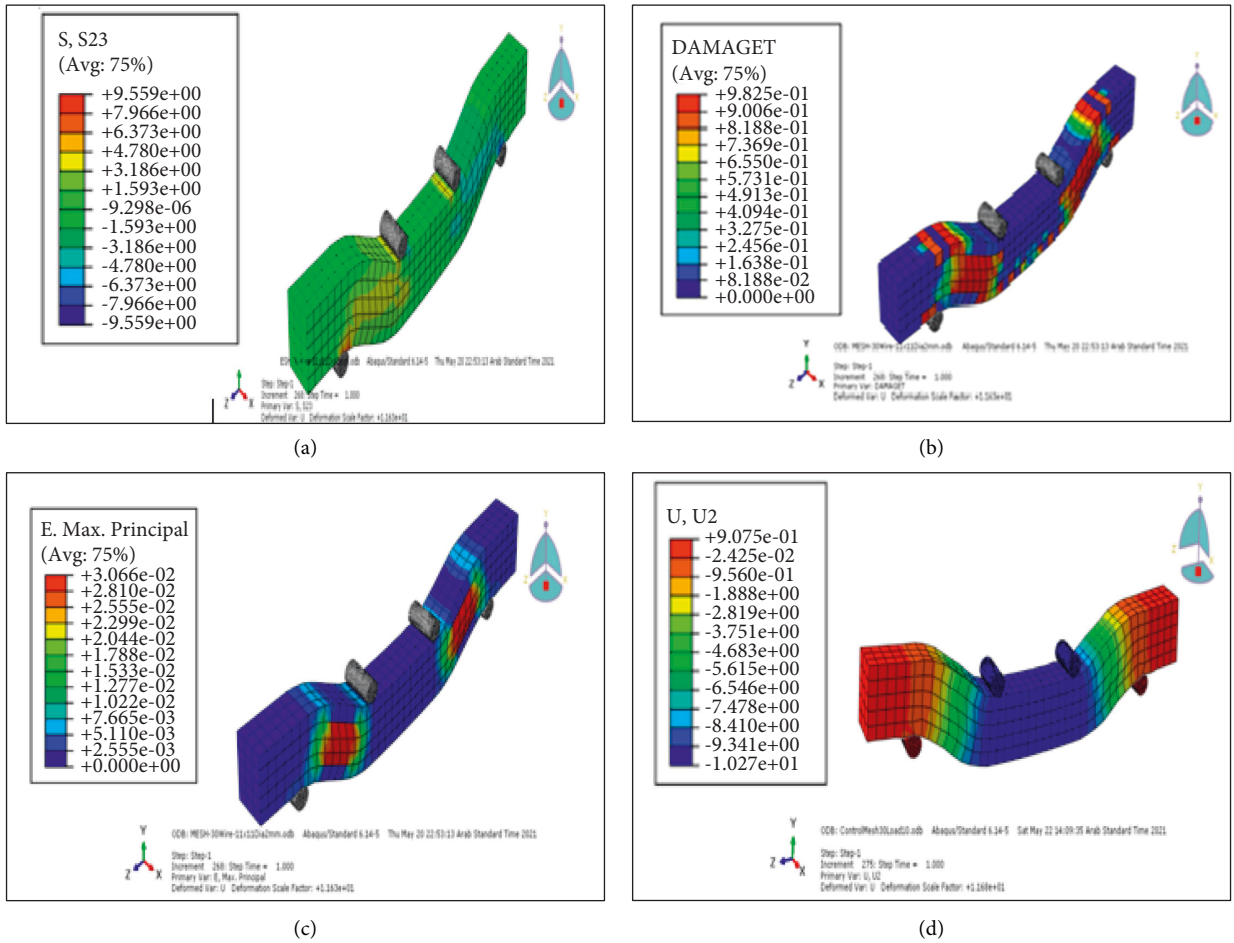

Figure 8: Sample FE results [(a) Maximum shear stress; (b) Damage pattern; (c) Principal strain; and (d) Maximum deflection].

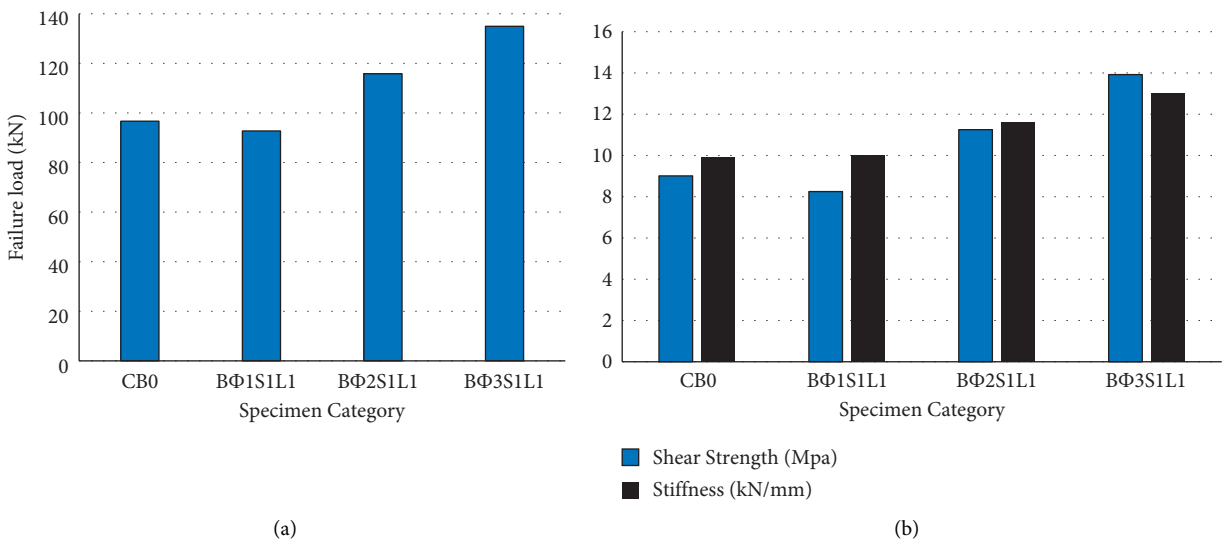

Figure 9: Effect of the diameter of wire mesh [(a) failure load and (b) shear strength and stiffness].

Figure 9(a) shows the influence of the diameter of wire mesh on the failure load of model specimens. As the diameter of the wire mesh increased from 1.5 mm to 2 mm and 1.5 mm to 2.5 mm, the failure load of the RC beam model specimen increased by 19.93% and 45.52%, respectively, keeping other study parameters constant. On another hand, Figure 9(b) illustrates the effect of the diameter of wire mesh on the shear strength and stiffness of RC beam specimens. The

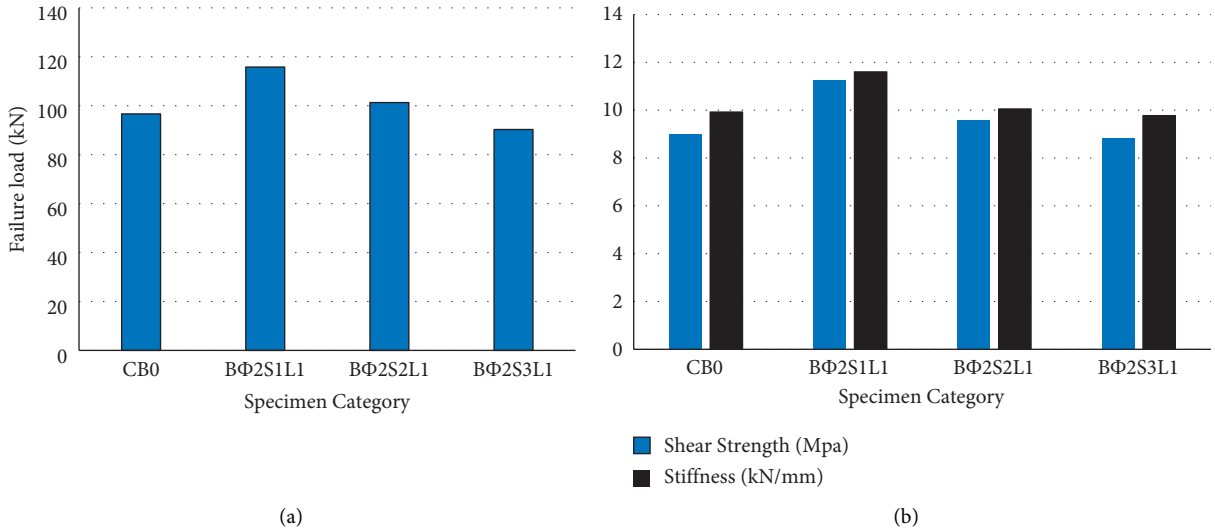

Figure 10: Effect of spacing of wire mesh [(a) Failure load, (b) Shear strength and stiffness].

shear strength and stiffness of the model specimens increased by 68.73% and 30%, respectively, as the diameter of the wire mesh increases from 1.5 mm to 2.5 mm. This testifies the significant effect of the diameter of wire mesh on the shear performance of RC beam under two-point loading.

3.1.2. Effects of Change in Spacing of Wire Mesh. In addition, the shear performance of the RC beam model specimens has been studied by considering different spacing of the wire mesh. The investigation confirmed a significant effect of spacing of wire mesh on the failure load, shear strength, and stiffness of the specimens. Figure 10(a) presents the ultimate failure load of RC beam specimens with different spacings of the wire mesh. As the spacing of the wire mesh increased from 8 mm × 8 mm to 11 mm × 11 mm and 8 mm × 8 mm to 15 mm × 15 mm, the ultimate failure load of the RC beam decreased by 12.52% and 22.04%, respectively, while the other parameters were kept constant. Under different spacings of the wire mesh, the shear strength and stiffness of RC beam specimens are presented in Figure 10(b). As the spacing of wire mesh increased from 8 mm × 8 mm to 15 mm × 15 mm, the specimen shear strength and stiffness decreased by 21.51% and 15.78%, respectively. This implies that, as the spacing of wire mesh increases, the failure load, shear strength, and stiffness of the specimens in decreased.

3.1.3. Effects of Change in Layers of Steel Wire Mesh. Further, the effect of layers of the wire mesh has been studied to access its influence on the shear performance of RC beam models as a study parameter. Layers of wire mesh have a tremendous effect on the shear performance of the model specimens. The study testified that as the number of layers of wire mesh increases, the ultimate failure load, shear strength, and stiffness of the models also increased. However, as the number of layers is greater than three, the effect/change on the performance of the RC beam becomes insignificant with no further change. Therefore, the wire mesh with three layers is the most economic and optimum to obtain the beam with good performance under two-point loading. Figure 11(a) shows the ultimate failure load of model specimens with a different number of layers of wire by keeping other study parameters constant. The ultimate failure load is increased by 60.05%, 73.68%, and 75.81%, as the number of layers of the wire mesh increased from one to two, one to three, and one to four, respectively. This result affirms the significance of the number of wire mesh on the shear performance of the RC beam. In another way, Figure 11(b) illustrates the effect of the number of layers of wire mesh on the shear capacity and stiffness of the model specimens. As the number of layers of wire mesh increased from one to four-layer, the shear capacity and stiffness of the model specimen increased by 108.2% and 50.42%, respectively.

3.1.4. Effects of Combination Wire Mesh with Stirrups. Under this category, the specimen with wire mesh only, stirrups only, and combination (wire mesh and stirrups) were prepared on equal weight criteria and modeled in FE simulation to access their shear performance under two-point loading. Figure 12(a) shows the failure load of the beam model under different forms of shear reinforcement. The ultimate load failure of the specimen with the wire mesh only is 19.8% greater than the specimen with stirrups only. On another hand, the ultimate load failure of the specimen with the combination (wire mesh and stirrups) is 19.5% greater than the specimen with stirrups only. Even the shear performance of the beam specimen with the wire mesh only is slightly greater than the beam specimen with the combination, on the same weight criteria, because of the high ductility behavior of the wire mesh. Figure 12(b) illustrates the significance of the different forms of shear reinforcement on the shear capacity and stiffness of beam models. The shear capacity and stiffness of beam specimen with wire mesh are 24.86% and 16.94% greater than specimen with stirrups only, respectively. The shear capacity and stiffness of beam specimen with wire mesh are 23.86% and 15.83% greater than specimen with stirrups only, respectively. This implies that under the same weight criteria, the shear performance of

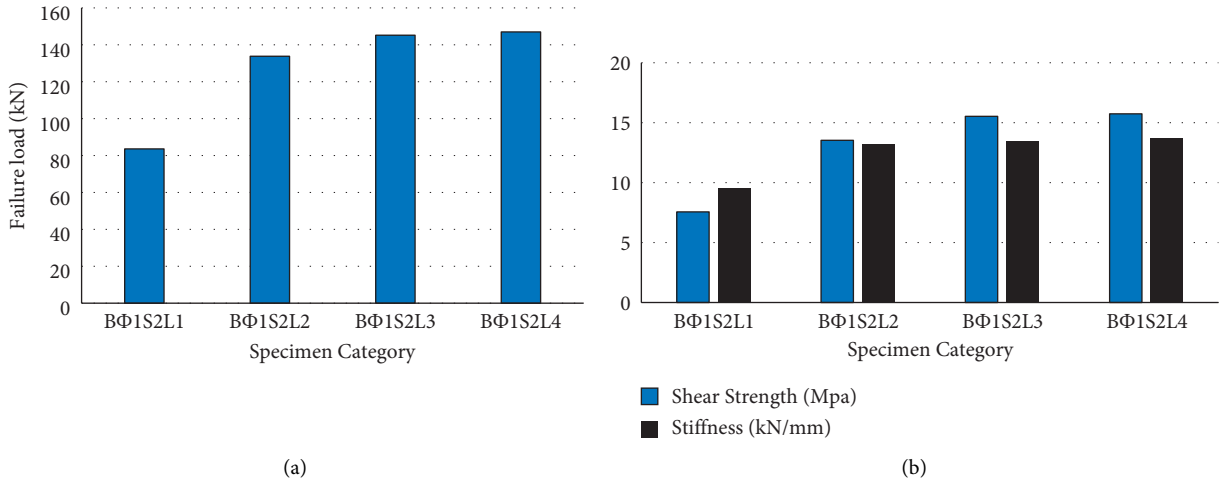

Figure 11: Effect of the number of layers of wire mesh [(a) Failure load, (b) Shear strength and stiffness].

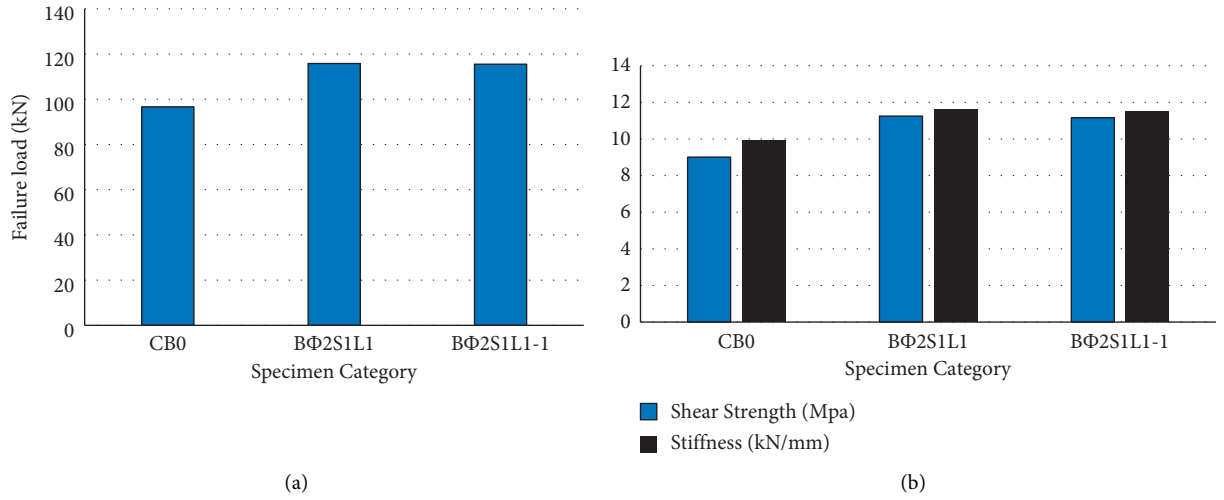

Figure 12: Effect of combination wire mesh with stirrups [(a) failure load, (b) shear strength and stiffness].

Table 6: Summary of FE simulation result.

Specimen	P_{ult}(KN)	Δ(mm)	V_u (Mpa)	Stiffness (KN/mm)	$P_{ult}/P_{ult.}r_{ef}$ (%)	$\Delta_{ult}/\Delta_{ult.}r_{ef}$ (%)	$V_u/V_{u.}r_{ef}$ (%)	$S_{tiffness}/S_{tiff.}r_{ef}$ (%)
CB0	96.67	9.74	9.01	9.92	100.00	100.00	100.00	100.00
BΦ1S1L1	92.73	9.27	8.25	10	95.92	95.17	91.56	100.81
BΦ2S1L1	115.81	9.99	11.25	11.6	119.80	102.57	124.86	116.94
BΦ3S1L1	134.94	10.46	13.92	13	139.59	107.39	154.50	131.05
BΦ3S1L2	146.11	10.76	15.42	13.58	151.14	110.47	171.14	136.90
BΦ3S1L3	153.57	10.57	16.81	14.55	158.86	108.52	186.57	146.67
BΦ1S2L1	83.6	10.1	7.56	9.58	86.48	103.70	83.91	96.57
BΦ2S2L1	101.3	10.38	9.56	10.05	104.79	106.57	106.10	101.31
BΦ3S2L1	122.46	10.74	11.12	10.97	126.68	110.27	123.42	110.58
BΦ1S2L2	133.8	10.1	13.53	13.23	138.41	103.70	150.17	133.37
BΦ1S2L3	145.2	10.8	15.53	13.44	150.20	110.88	172.36	135.48
BΦ1S2L4	146.98	10.2	15.74	14.41	152.04	104.72	174.69	145.26
BΦ2S3L1	90.29	8.5	8.83	9.77	93.40	87.27	98.00	98.50
BΦ3S3L2	141.15	9.37	14.06	15.06	146.01	96.20	156.05	151.81
BΦ2S1L1-1	115.51	9.93	11.16	11.49	119.49	101.95	123.86	115.83

the specimen with wire mesh only or combination is greater than specimen with stirrups only.

The summary of all model specimens has been presented in Table 6, which contains failure load, deflection, shear capacity, and stiffness.

3.2. Sensitivity Analysis. Furthermore, sensitivity analysis was performed in MS Excel for each dependent variable to evaluate the effect of independent variables. This was important to know how much independent variables influence dependent variables both individually and in combination.

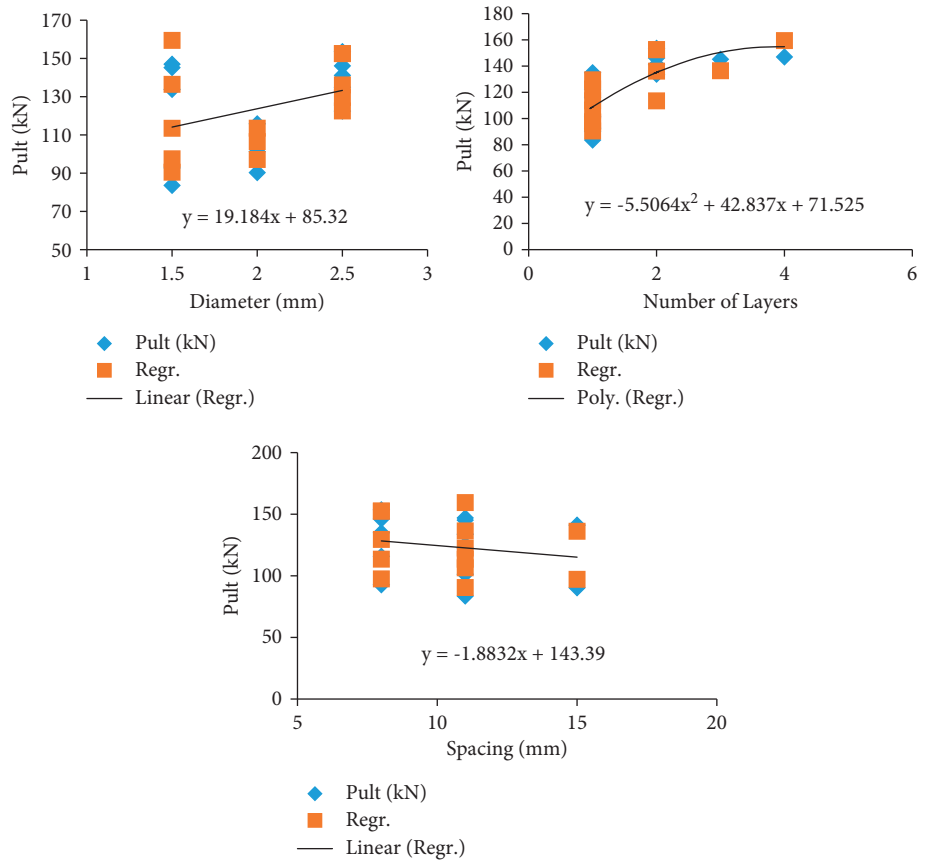

Figure 13: Predicted equation for ultimate failure load with the respective independent variable.

Figure 13 illustrates the predicted equation of ultimate load failure with respective independent variables (diameter, number of layers and spacing of wire mesh) individually. There is a positive relationship between ultimate failure load and independent variables like diameter and the number of layers of wire mesh. However, as the layers become greater than 3, the line is almost horizontal, which means no change in shear performance. On the other hand, there is a negative relationship between spacing wire mesh and the ultimate failure load.

Equation (17) presents the predicted linear equation obtained by regression analysis, which is used to predict the ultimate failure load by considering independent variables in combination.

$$\text{Failure load} = 32.04\Phi + 22.98l - 2.34s + 45.19, \quad (17)$$

where failure load is in kN, Φ is the diameter of wire mesh in mm, l is the number of layers of wire mesh, and s is the spacing between the wire mesh.

4. Conclusion

The study was focused on the shear performance of the RC beam with wire mesh as shear reinforcement in terms of ultimate failure load, shear capacity, and stiffness by considering different independent variables like diameter, spacing, the number of layers of wire mesh, and its combination with stirrups. A numerical investigation was undertaken using FE simulation with Abaqus Software. Based on the FE simulation the following conclusions were drawn:

(a) As the diameter of wire mesh increases, the ultimate load failure, shear capacity, and stiffness of RC beam specimens are also increased. As the diameter of wire mesh increases from 1.5 mm to 2.5 mm, the ultimate load failure, the shear strength, and the stiffness of the beam increased by 45.52%, 68.73%, and 30%, respectively, keeping other study parameters constant.

(b) In another way, as the spacing of wire mesh increases, the ultimate load failure, shear capacity, and stiffness of the RC beam model specimen are decreased. As the spacing of wire mesh increases from 8 mm × 8 mm to 15 mm × 15 mm, the ultimate load failure, shear strength, and stiffness of the beam specimen decrease by 22.04%, 21.51%, and 8.44%, respectively, keeping other study parameters constant.

(c) The ultimate failure load, shear capacity, and stiffness of the specimen are increased as the number of layers of wire mesh increases. However, as the number of layers of wire mesh becomes greater than three, the change in shear performance becomes insignificant. Therefore, three layers of wire mesh are the most economic and optimum in improving the shear performance of the RC beam.

(d) Under the same weight criteria, the shear performance of beam model with wire mesh only and combination (wire mesh and stirrups) as shear reinforcement is greater than specimen with stirrups only. In addition, the shear performance of beam specimen with wire mesh only is slightly greater than the beam specimen with the combination (wire mesh and stirrups) because of the high ductility behavior of wire mesh.

Data Availability

All required data are available in the paper.

Conflicts of Interest

The authors declare that there are no conflicts of interest regarding the study.

Acknowledgments

The authors would like to thank all those who shared their experiences and resources in performing the study.

References

[1] A. C. I. Committee, vol. , 2018, pp 549Report on Ferrocement, pp. 549R–618R, American Concrete Institute, Farmington Hills.

[2] H. Eskandari and A. Madadi, "Investigation of ferrocement channels using experimental and finite element analysis," *Engineering Science and Technology, an International Journal*, vol. 18, no. 4, pp. 769–775, 2015.

[3] M. A. Al-Kubaisy and M. Zamin Jumaat, "Flexural behaviour of reinforced concrete slabs with ferrocement tension zone cover," *Construction and Building Materials*, vol. 14, no. 5, pp. 245–252, 2000.

[4] B. Li and E. S. S. Lam, "Influence of interfacial characteristics on the shear bond behaviour between concrete and ferrocement," *Construction and Building Materials*, vol. 176, pp. 462–469, 2018.

[5] I. G. Shaaban and O. A. Seoud, "Experimental behavior of full-scale exterior beam-column space joints retrofitted by ferrocement layers under cyclic loading," *Case Studies in Construction Materials*, vol. 8, pp. 61–78, 2018.

[6] M. T. Kazemi and R. Morshed, "Seismic shear strengthening of R/C columns with ferrocement jacket," *Cement and Concrete Composites*, vol. 27, no. 7-8, pp. 834–842, 2005.

[7] Y. B. I. Shaheen, A. M. Mahmoud, and H. M. Refat, "Structural performance of ribbed ferrocement plates reinforced with composite materials," *Structural Engineering & Mechanics*, vol. 60, no. 4, pp. 567–594, 2016.

[8] C. R. Vol, C. Ca, E. Science, and R. April, "Thin webbed sections," *Cement and Concrete Research*, vol. 25, no. 5, pp. 969–979, 1995.

[9] H. H. Nassif and H. Najm, "Experimental and analytical investigation of ferrocement-concrete composite beams," *Cement and Concrete Composites*, vol. 26, no. 7, pp. 787–796, 2004.

[10] P. Paramasivam, C. T. E. Lim, and K. C. G. Ong, "Strengthening of RC beams with ferrocement laminates," *Cement and Concrete Composites*, vol. 20, no. 1, pp. 53–65, 1998.

[11] C. E. Chalioris and E. F. Sfiri, "Shear performance of steel fibrous concrete beams," *Procedia Engineering*, vol. 14, pp. 2064–2068, 2011.

[12] A. M. Erfan and T. A. El-Sayed, "Structural shear behavior of composite box beams using advanced innovated materials," *Journal of Engineering Research and Reports*, vol. 5, pp. 1–14, 2019.

[13] A. M. Erfan and T. A. El-sayed, "Shear strength of ferrocement composite box section concrete beams," *Rice & Wheat Straw Ashes As A cement replacement materials*, vol. 10, no. 5, pp. 260–279, 2019.

[14] T. A. El-Sayed, "Axial compression behavior of ferrocement geopolymer hsc columns," *Polymers*, vol. 13, no. 21, pp. 3789–21, 2021.

[15] G. J. Al-Sulaimani, I. A. Basunbul, and E. A. Mousselhy, "Shear behavior of ferrocement box beams," *Cement and Concrete Composites*, vol. 13, no. 1, pp. 29–36, 1991.

[16] T. A. El-Sayed and A. M. Erfan, "Improving shear strength of beams using ferrocement composite," *Construction and Building Materials*, vol. 172, pp. 608–617, 2018.

[17] A. Inc, *ABAQUS Version 6.10-1 Analysis User's Manual*, vol. III, pp. 1–10, Dassault Systèmes Simulia Corp, Johnston, RI, 2017.

[18] European Committee for Standardization, *Eurocode 2: Design of concrete Structures - Part 1: General Rules and Rules for buildings November*, vol. 1, European Committee for Standardization, Brussels, 2002.

[19] J. da Costa, "Structural properties of steel-concrete composite joints," *Faculty of Sciences, Technology and Communication*, University of Luxembourg, Luxembourg, 2018.

[20] W. Ren, L. H. Sneed, Y. Yang, and R. He, "Numerical simulation of prestressed precast concrete bridge deck panels using damage plasticity model," *International Journal of Concrete Structures and Materials*, vol. 9, no. 1, pp. 45–54, 2015.

[21] G. A. Hegemier, R. O. Nunn, and S. K. Arya, "Behavior of concrete masonry under biaxial stresses," *ACI Structural Journal*, vol. 66, pp. 656–666, 1978.

[22] J. Lubliner, J. Oliver, S. Oller, and E. Oñate, "A plastic-damage model for concrete," *International Journal of Solids and Structures*, vol. 25, no. 3, pp. 299–326, 1989.

[23] T. Wang and T. T. C. Hsu, "Nonlinear finite element analysis of concrete structures using new constitutive models," *Computers & Structures*, vol. 79, no. 32, pp. 2781–2791, 2001.

[24] A. Feyissa and G. Kenea, "Performance of shear connector in composite slab and steel beam with reentrant and open trough profiled steel sheeting," *Advances in Civil Engineering*, vol. 2022, Article ID 5010501, 14 pages, 2022.

[25] A. Hamicha and G. Kenea, "Investigation on the effect of geometric parameter on reinforced concrete exterior shear wall-slab connection using finite element analysis," *Advances in Civil Engineering*, vol. 2022, Article ID 4903650, 17 pages, 2022.

[26] D. Elavarasi and A. Sumathi, "Behaviour of reinforced concrete beams with wire mesh as shear reinforcement," *International Journal of Innovative Technology and Exploring Engineering*, vol. 8, no. 12, pp. 781–784, 2019.